THE ASTROPHYSICAL JOURNAL, 467:L53–L56, 1996 August 20


# ANGULAR SIZES OF FAINT FIELD DISK GALAXIES: INTRINSIC LUMINOSITY EVOLUTION

LAURA CAYÓN AND JOSEPH SILK
Astronomy Department and Center for Particle Astrophysics, University of California, Berkeley, CA 94720
AND
STÉPHANE CHARLOT
Institut d'Astrophysique du CNRS, 98 bis boulevard Arago, 75014 Paris, France
*Received 1996 April 5; accepted 1996 June 6*

## ABSTRACT

In order to explain the small scale lengths detected in the recent deep field observations performed from large ground-based telescopes and from the *Hubble Space Telescope*, we investigate the predictions at high redshifts for disk galaxies that formed by infall. Changes with redshift in the observed properties of field galaxies are directly related to the evolution of the disks and of the stellar populations. We see that changes in the rest-frame luminosity of a galaxy induce smaller values of half-light radii than are predicted assuming no evolution. Comparisons are presented with two observed samples from Mutz et al. and Smail et al.

*Subject headings:* Galaxy: evolution — galaxies: formation

## 1. INTRODUCTION

Studies of the faint field population of galaxies have traditionally been based on number counts and analyses of redshift distributions. Distinguishing Hubble types and/or measuring the morphological characteristics of these galaxies has become feasible only with the advent of new era telescopes. Observations from the largest ground-based telescope have provided data on the sizes of faint field galaxies (Smail et al. 1995), while more refined morphological classification can be achieved using high-resolution observations with the *Hubble Space Telescope* (*HST*) (Mutz et al. 1994; Casertano et al. 1995; Driver, Windhorst, & Griffiths 1995a; Glazebrook et al. 1995; Driver et al. 1995b; Schade et al. 1995; Abraham et al. 1996).

At faint magnitudes $I \approx 22$ and $R \approx 26$ (expected median redshift greater than 0.5; see, e.g., Lilly et al. 1995), the dominant field population consists of very small disk systems with mean scale length of $\sim 0\farcs2$–$0\farcs3$ (Casertano et al. 1995; Smail et al. 1995). The corresponding drop in median galaxy size with increasing magnitude and redshift is faster than predicted by assuming a fixed intrinsic angular size of galaxies (Mutz et al. 1994; Im et al. 1995; Smail et al. 1995). Hence, faint distant galaxies are either intrinsically smaller or their emission is more concentrated toward the nuclear regions than that of low-redshift bright galaxies. In fact, the evolution of stellar populations in galaxies is likely to affect the intrinsic surface brightness profile and therefore the observed half-light radius.

Studies of our own Galaxy have converged on a model for global star formation in which the Galaxy formed inside out, leading to predictions of star formation rate, gas surface density, and metallicity as functions of time and galactic radius; see, e.g., Lacey & Fall (1985) and Wang & Silk (1994). Prantzos & Aubert (1995) have demonstrated that a robust and generic model contains the following ingredients: a rate of star formation that is proportional to the product of gas surface density and differential rotation rate, and infall of unenriched gas during the first few gigayears. The radial dependence of the star formation prescription on total gas surface density, and via a star formation threshold on differential rotation rate, has been verified for a sample of nearby spirals in a study of H$\alpha$ emission from prominent H II regions by Kennicutt (1989). Because the rotation curves are flat throughout most of the star-forming regions of disks, it follows that disks must have formed inside out. Hence, small scale lengths are expected at early ages.

In this Letter, we consider idealized disk galaxy models with infall to explore the influence of the radial dependence of the star formation rate on the observed angular sizes of distant galaxies. In § 2 we present models that reproduce the characteristics of local disk galaxies of various morphological types and compute the predicted evolution of the intrinsic surface brightness profiles with redshift. In § 3 we compare our models with recent observations by Mutz et al. (1994) and Smail et al. (1995). We conclude from this simple but quantitative analysis that intrinsic luminosity evolution provides a potential explanation for the decrease in the angular size of faint galaxies observed in deep surveys. In all the calculations presented below, we adopt a fixed Hubble constant of $H_0 = 50$ km s$^{-1}$ Mpc$^{-1}$.

## 2. DISK GALAXIES: INFALL FORMATION

We first describe infall formation models that reproduce the observed characteristics of present-day disk galaxies of various Hubble types. Models with infall are favored by recent studies of chemical evolution in the Galactic disk that are consistent with the observed gas and star surface densities, metallicity profile, and star formation rate (SFR) (Ferrini et al. 1994; Dopita & Ryder 1994; see Prantzos & Aubert 1995 for a detailed comparative analysis). Prantzos & Aubert conclude that a phenomenological model satisfying the observational requirements is one with infall in which the SFR depends on radius and time following a Schmidt-type law:

$$\mathrm{SFR}(r, t) = (1 - R)^{-1} \frac{\Sigma_g(r, t)}{\tau_g(r)} M_\odot \ \mathrm{pc}^{-2} \ \mathrm{Gyr}^{-1}, \quad (1)$$

where $R \approx 0.32$ is the returned fraction of mass that was formed into stars, $\Sigma_g(r, t)$ is the gas surface density at radius $r$ and age $t$, and $\tau_g(r) = [0.3(1 - R)(r_\odot/r)]^{-1}$ Gyr is the gas

consumption timescale ($r_\odot = 8.5$ kpc). This model explains many properties of our Galaxy both as a function of radius and of age. Equation (1) relies on the instantaneous recycling approximation, which must be relaxed in studies of the metallicity in the inner radii of disks (see, e.g., Prantzos & Aubert 1995). Since we are interested here only in galactic luminosity and size evolution, our results are not appreciably affected by this approximation. The evolution of gas surface density in the infall disk model can be written

$$\frac{d\Sigma_g(r, t)}{dt} = -\mathrm{SFR}(r, t)(1 - R) + f(r, t), \qquad (2)$$

where $f(r, t) \propto \exp[-t/\tau_f(r)]$ is the infall rate of metal-free gas with characteristic timescale $\tau_f(r)$. We normalize the infall rate to the total surface density $\Sigma_{\rm tot}$ of stars plus gas observed at the age $T = 13.5$ Gyr. Solving equation (2) for the evolution of the gas surface density, we obtain

$$\Sigma_g(r, t) = \Sigma_{\rm tot}(r, T)\,\frac{\exp[-t/\tau_g(r)] - \exp[-t/\tau_f(r)]}{\{1 - [\tau_f(r)/\tau_g(r)]\}\{1 - \exp[-T/\tau_f(r)]\}}. \qquad (3)$$

So far, we have considered a pure disk model, for which the main free parameters are the infall timescale, $\tau_f(r)$, and the total surface density distribution of stars plus gas at time $T$, $\Sigma_{\rm tot}(r, T)$. We now adjust these parameters for galaxies of different Hubble types (Sb, Sbc-Sc, and Sd-Im) by combining the disk model with a type-dependent bulge component to reproduce the observed spectral energy distributions, surface brightness profiles, bulge-to-total luminosity ratios, and Scalo parameters (i.e., the ratio of present-to-past averaged SFR) of nearby galaxies. To achieve this, we compute the spectrophotometric properties of model galaxies, using the latest version of the Bruzual-Charlot stellar population synthesis models (Charlot, Worthey, & Bressan 1996). The initial mass function is assumed to be a power law with the Salpeter slope and upper and lower cutoffs at 125 and 0.1 $M_\odot$, respectively. We fix the metallicity at the solar value. This should be a good approximation at most ages but may slightly underestimate (by less than 20%) the luminosity at the youngest ages because metal-poor stars are somewhat more luminous than metal-rich ones (Bruzual & Charlot 1996).

We adopt constant infall timescales of $\tau_f = 3$ Gyr, 7 Gyr, and $\infty$ for the model Sb, Sbc-Sc, and Sd-Im galaxies, respectively. For all galaxy types, at $T = 13.5$ Gyr, the disk component is assumed to have the total surface density distribution of stars plus gas observed in the disk of the Galaxy (Fig. 1 of Prantzos & Aubert 1995). We then define the surface density of stars plus gas inside the bulge (at $T = 13.5$ Gyr) as well as the bulge radius for the different types by requiring that (1) the bulge-to-total luminosity ratios of Sb, Sbc-Sc, and Sd-Im galaxies be 0.20, 0.13, and 0.0, respectively (Kennicutt, Tamblyn, & Congdon 1994; Ferguson & McGaugh 1995) and (2) the bulge and disk surface brightness profiles fit exponential laws with a type-independent scale length ratio of ~0.1 (Andredakis, Peletier, & Balcells 1995; Courteau, de Jong, & Broeils 1996). The model galaxy bulges at $T = 13.5$ Gyr are assumed to have null gas surface density and exponential stellar surface density profiles normalized to fit the adopted disk profiles at bulge radii of 2 and 1.5 kpc for the Sb and Sbc-Sc types, respectively. The validity of the models is checked by comparing the model spectra at age 13.5 Gyr with those of present-day Sb, Sbc-Sc, and Sd-Im galaxies. The spectral energy distribution is essentially controlled by the Scalo parameter, which is observed to range from about 0.01 in Sa galaxies to over 1.0 in late-type spiral galaxies (see, e.g., Kennicutt et al. 1994). The Scalo parameters produced by the adopted Sb, Sbc-Sc, and Sd-Im models are ~0.45, ~0.7, and ~1.2, respectively. The model Sb, Sbc-Sd, and Sd-Im galaxies computed in this way have absolute $B$ magnitudes at $T = 13.5$ Gyr of about −19.5, −19.7, and −19.9, respectively.

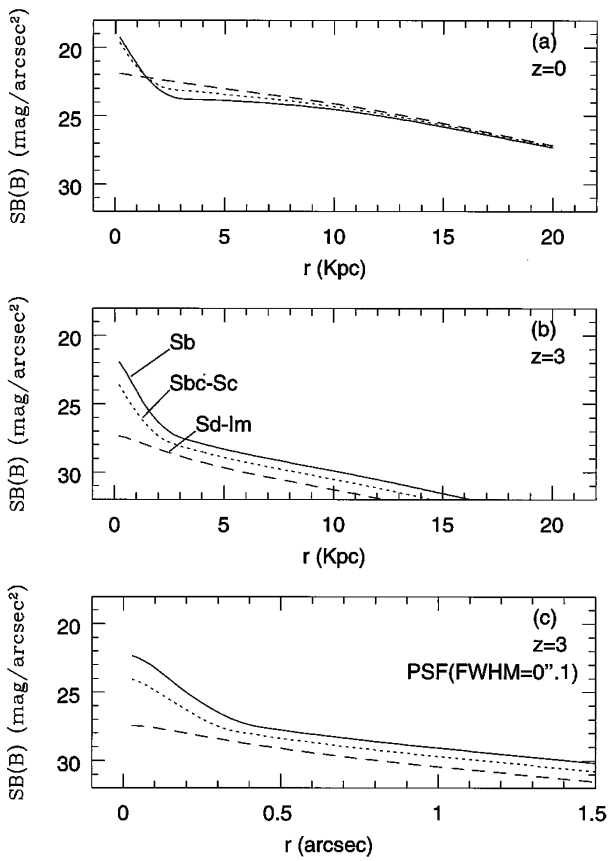


FIG. 1.—Apparent surface brightness profiles as a function of physical radius for Sb (*solid line*), Sbc-Sc (*dotted line*), and Sd-Im (*dashed line*) model galaxies with infall at (*a*) $z = 0$ and (*b*) $z = 3$, for $\Omega = 1$, $H_0 = 50$ km s$^{-1}$ Mpc$^{-1}$, and a formation redshift $z_f = 10$. (*c*) Same as (*b*) but as a function of angular radius and after convolving the model profile with a PSF of FWHM = 0".1.

The predicted rest-frame surface brightness profiles at an age of 13.5 Gyr are displayed in Figure 1*a* for the three galaxy types. Figure 1*b* shows that the evolution of the underlying stellar population implies significant changes in the surface brightness profiles. At $z = 3$, the central regions of the Sb galaxy are intrinsically significantly brighter than at $z = 0$, while those of the Sd-Im galaxy are only slightly brighter. The reason for this is that early-type disk galaxies with short timescales of star formation fade more rapidly than late-type ones. As a result, from $z = 0$ to $z = 3$, the apparent surface brightness of Sb, Sbc-Sc, and Sd-Im galaxies drops by about 3, 4, and 5 mag arcsec$^{-2}$, respectively. As we shall see below, these changes in the surface brightness profiles of disk galaxies with infall have important consequences for the observed angular sizes and half-light radii. In Figure 1*c*, we have convolved the predicted profiles with an observational point-

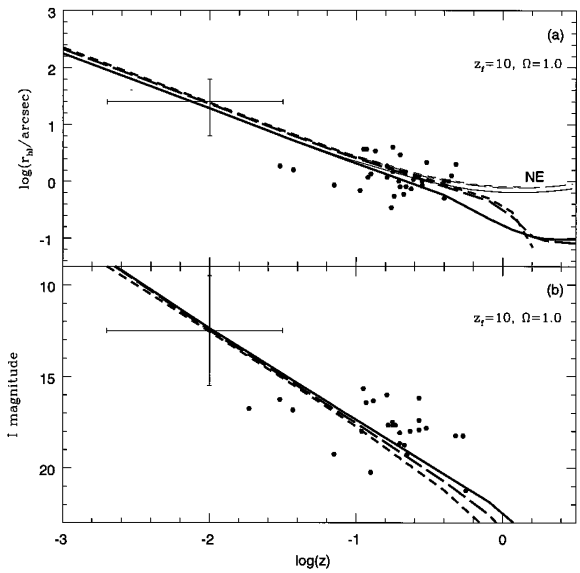


FIG. 2.—Observed (*a*) half-light radius and (*b*) *I* magnitude as a function of redshift. The circles are from the observed sample of faint disk galaxies by Mutz et al. (1994), while large crosses indicate the range of properties of nearby disk galaxies (Mathewson et al. 1992). The curves show the predictions for the Sb (*solid*), Sbc-Sc (*long-dashed*), and Sd-Im (*short-dashed*) models both with (*thick*) and without (*thin*) intrinsic luminosity evolution. Cosmological parameters are the same as in Fig. 1.

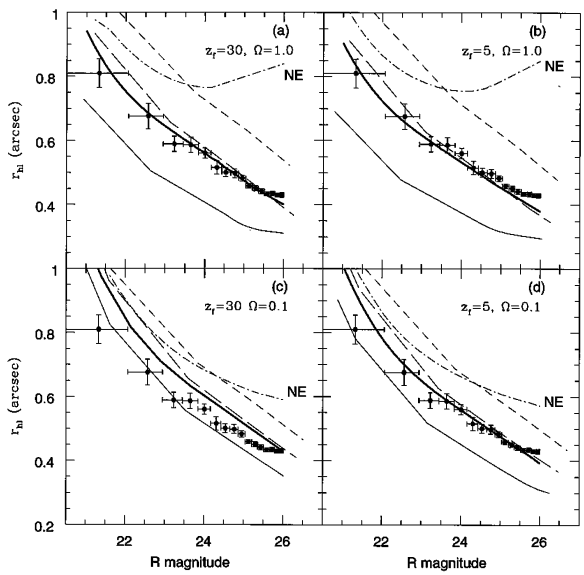


FIG. 3.—Observed half-light radius vs. apparent *R* magnitude. The data are from the observations of Smail et al. (1995), filled circles corresponding to medians of 401 galaxies, horizontal error bars to the extent of the magnitude bin, and vertical error bars to the 95% confidence limits (see original paper for detail). Model predictions are shown for four different cosmologies, (*a*) $z_f = 30$, $\Omega = 1.0$, (*b*) $z_f = 5$, $\Omega = 1.0$, (*c*) $z_f = 30$, $\Omega = 0.1$, and (*d*) $z_f = 5$, $\Omega = 0.1$. Solid (thin) lines denote the predicted half-light radii vs. *R* magnitude for the Sb model. Long-dashed lines refer to the Sbc-Sc model, and short-dashed lines correspond to the Sd-Im model predictions. Evolution of the intrinsic luminosity has been considered in these predictions. The thick solid lines correspond to the weighted average of the half-light radius predicted in the different cosmologies for the disk field population. Thin dashed-dotted lines show corresponding weighted averages for the models with fixed half-light radius (no intrinsic luminosity evolution).

spread function (PSF) of FWHM 0″.1. We note the consistency between our predicted profiles for forming bulge/disk systems and the profiles fitted to star-forming galaxies at redshifts greater than 3 (Giavalisco, Steidel, & Macchetto 1996).

## 3. COMPARISON WITH OBSERVATIONS

Sizes of faint field galaxies have been measured in high-resolution *HST* images as part of the Medium Deep Survey (MDS) project (Griffiths et al. 1994; Mutz et al. 1994; Casertano et al. 1995; Phillips et al. 1995; Forbes et al. 1995), which allow morphological classification to $I \lesssim 22$ mag and, to even fainter magnitudes ($R < 27$ mag), in ground-based studies using the Keck telescope (Smail et al. 1995). Even though ground-based studies do not allow morphological classification of galaxies at these faintest magnitudes, a comparison with the models presented in § 2 is also important because disk galaxies are expected to dominate the field population (see below). In comparing our models with observations, we account for the effect of the PSF and specific magnitude measurement scheme adopted (aperture or isophotal). The convolution with a PSF has the effect of increasing the inferred half-light radii. We further assume for simplicity that the simulated galaxies are observed face-on. We now present results of comparisons of the models with the observations of Mutz et al. (1994) and Smail et al. (1995).

Consider first data from the *HST* MDS project, taken with the Wide Field Planetary Camera in two filters *V*(5550 Å) and *I*(8930 Å) (Mutz et al. 1994). These include isophotal magnitudes measured down to outer isophotes of $SB(V) \sim 27.0$ mag arsec$^{-2}$ and $SB(I) \sim 25.5$ mag arcsec$^{-2}$ for 33 morphologically identified disk galaxies at $0.02 \lesssim z \lesssim 0.6$ (PSF of FWHM ~ 0″.1). In Figure 2, we compare the observed evolution of half-light radius and *I* magnitude as a function of redshift with the predictions of the various disk models. We have assumed that galaxies formed at a redshift $z_f = 10$ in an $\Omega = 1$ universe, but similar results would be obtained for cosmologies with $z_f = 5$–30 and $\Omega = 0.1$–1.0. Also indicated by large crosses in the two panels are the observed properties of nearby disk galaxies from the sample of Mathewson, Ford, & Buchhorn (1992). The predicted angular sizes and *I* magnitudes are consistent with the mean of the observations at low and high redshifts, although the model *I* magnitudes may be slightly fainter than the MDS magnitudes at the highest redshifts. Figure 2*a* also shows that at $z \gtrsim 1$, the predicted half-light radius of Sd-Im galaxies becomes smaller than that of earlier type disks. The reason for this is that Sd-Im galaxies have the faintest central surface brightness (Fig. 1*b*), and hence only light from the very central part of the disk satisfies the isophotal magnitude selection. For comparison, we also show in Figure 2*a* the predictions of no-evolution models assuming constant intrinsic luminosity profiles of galaxies. Even though evolution affects only mildly the predictions in the observed range of redshifts, it makes considerable difference at $z \gtrsim 1$.

Next, we consider the sample of galaxies observed in the *V*, *R*, and *I* bands by Smail et al. (1995) with the Keck Telescope. Following Smail et al. (1995), we compute model *R* magnitudes by adopting the largest of a fixed 1″.5 diameter aperture or isophotal diameter down to a surface brightness limit of $SB(R) \approx 28.3$ mag arcsec$^{-2}$. The adopted seeing FWHM is 0″.6. The observed mean half-light radii are plotted as a function of *R* magnitude in Figure 3 together with model predictions for four different combinations of $z_f$ and $\Omega$. The

observational relation is more tightly defined than the radius-redshift and magnitude-redshift relations considered previously (Fig. 2) because it is based on a much larger sample of objects. As a result, the differences in the predictions for the various disk Hubble types are larger than the observational uncertainties.

To make a more meaningful comparison with the observations, we have estimated weighted average values of the predicted half-light radius of the disk population as a function of $R$ magnitude. We assume that 70% of the local field population is accounted for by disk galaxies with ratios Sb:Sbc-Sc:Sd-Im $\sim 25\%:25\%:20\%$ (Ferguson & McGaugh 1995) independent of redshift. We do not include here the contribution to the average half-light radius values by elliptical and S0 galaxies, but a recent morphological analysis of ultradeep *HST* images suggests that early-type galaxies should account for only a minority of the observed galaxies at the faintest magnitudes (Abraham et al. 1996). Although a large fraction of galaxies at $I \gtrsim 25$ mag in these observations appear to be peculiar, irregular, or merging systems, this may be in part a bias due to our viewing these systems in rest-frame $U/B$ bands. We then expect the high-redshift predictions of our models, presented in terms of half-light radii rather than detailed profile fitting, to be a reasonable representation of disk sizes in young or even forming galaxies. Figure 3 shows results both including and not including intrinsic luminosity evolution. The differences in the shapes of the $r_{hl}$ curves are especially striking at the faintest $R$ magnitudes. The predictions of models with evolution to $R \approx 26$ depend moderately on the assumed redshift of formation and density parameter. The dependence is stronger for Sb galaxies than for Sd-Im galaxies because earlier type galaxies have shorter timescales of star formation and fade more significantly as they age. As expected, predictions of models without evolution do not fit the data at faint magnitudes, and they depend more markedly on $\Omega$. We interpret the overall agreement between predictions and observations in Figure 3 as an indication that, within the framework of disk galaxy formation by infall, intrinsic luminosity evolution should be included to explain, at least partially, the small observed sizes of disk galaxies at faint magnitudes.

In summary, we have applied infall formation models to simulate the radial dependence of the SFR in different Hubble types of disk galaxies. The inside-out formation of galaxies in these models, together with the chemical evolution of their stellar populations, change the rest-frame surface brightness profiles of the simulated galaxies as they evolve. Earlier types are more affected by this intrinsic luminosity evolution. Observational constraints for the samples analyzed in Mutz et al. (1994) and in Smail et al. (1995) were imposed on the modeled galaxies. As expected and shown in Figures 2 and 3, *infall models including rest-frame luminosity evolution predict angular sizes smaller than models with fixed half-light radius*. Moreover, such models can explain the clear trend toward very small sizes observed at faint magnitudes and high redshift. The simple models considered here are based primarily on fitting the properties of nearby galaxies and provide a robust description of present-epoch star formation rates and luminosity profiles. Evolving these models backward in time is the most direct approach toward interpreting data on distant galaxies. It would be of considerable interest to refine the predictions of our models by including a more realistic mix of galaxy types and luminosities in order to make a more detailed comparison with the characteristics of the population observed in the Hubble Deep Field sample.

We acknowledge Ian Smail for providing us with the data presented in Figure 3. This work was supported in part by a grant from NASA.

REFERENCES

Abraham, R. G., Tanvir, N. R., Santiago, B. X., Ellis, R. S., Glazebrook, K., & van den Bergh, S. 1996, astro-ph/9602044
Andredakis, Y. C., Peletier, R. F., & Balcells, M. 1995, MNRAS, 275, 874
Bruzual, G. A., & Charlot, S. 1996, in preparation
Casertano, S., Ratnatunga, K. U., Griffiths, R. E., Im, M., Neuschaefer, L. W., Ostrander, E. J., & Windhorst, R. A. 1995, ApJ, 453, 599
Charlot, S., Worthey, G., & Bressan, A. 1996, ApJ, 457, 625
Courteau, S., de Jong, R. S., & Broeils, A. H. 1996, ApJ, 457, L73
Dopita, M., & Ryder, S. 1994, ApJ, 430, 163
Driver, S. P., Windhorst, R. A., & Griffiths, R. E. 1995a, ApJ, 453, 48
Driver, S. P., Windhorst, R. A., Ostrander, E. J., Keel, W. C., Griffiths, R. E., & Ratnatunga, K. U. 1995b, ApJ, 449, L23
Ferguson, H. C., & McGaugh, S. S. 1995, ApJ, 440, 470
Ferrini, F., Molla, M., Pardi, M., & Diaz, A. 1994, ApJ, 427, 745
Forbes, D. A., Phillips, A. C., Koo, D. C., & Illingworth, G. D. 1995, astro-ph/9511014
Giavalisco, M., Steidel, C. C., & Macchetto, F. 1996, ApJ, in press
Glazebrook, K., Ellis, R. S., Santiago, B., & Griffiths, R. E. 1995, MNRAS, 275, L19
Griffiths, R. E., et al. 1994, ApJ, 437, 67
Im, M., Casertano, S., Griffiths, R. E., & Ratnatunga, K. U. 1995, ApJ, 441, 494
Kennicutt, R. C. 1989, ApJ, 344, 685
Kennicutt, R. C., Tamblyn, P., & Congdon, C. W. 1994, ApJ, 435, 22
Lacey, C. G., & Fall, S. M. 1985, ApJ, 290, 154
Lilly, S. J., Tresse, L., Hammer, F., Crampton, D., & Le Fèvre, O. 1995, ApJ, 455, 108
Mathewson, D. S., Ford, V. L., & Buchhorn, M. 1992, ApJS, 81, 413
Mutz, S. B., Windhorst, R. A., Schmidtke, P. C., Psacarelle, S. M., Griffiths, R. E., Ratnatunga, K., Im, M., & Neuschaefer, L. W. 1994, ApJ, 434, L55
Phillips, A. C., Bershady, M. A., Forbes, D. A., Koo, D. C., Illingworth, G. D., Reitzel, D. B., Griffiths, R. E., & Windhorst, R. A. 1995, ApJ, 444, 21
Prantzos, N., & Aubert, O. 1995, A&A, 302, 69
Schade, D., Lilly, S. J., Crampton, D., Hammer, F., Le Fevre, O., & Tresse, L. 1995, ApJ, 451, L1
Smail, I., Hogg, D. W., Yan, L., & Cohen, J. G. 1995, ApJ, 449, L105
Wang, B. Q., & Silk, J. 1994, ApJ, 427, 759